Casting Fe–Al-based intermetallics alloyed with Li and Ag

M. Villagomez-Galindo
Facultad de Ingeniería Mecánica, Universidad Michoacana de San Nicolás de Hidalgo, C.P. 58000, Morelia, México; and Department of Mechanical Engineering (EUETIB), Universitat Politécnica de Catalunya, 08034 Barcelona, Spain

G. Carbajal-De la Torre
Facultad de Ingeniería Mecánica, Universidad Michoacana de San Nicolás de Hidalgo, C.P. 58000, Morelia, México

J.C. Romo-Castañeda
Facultad de Química, Universidad Nacional Autónoma de México, C.P. 04510 Ciudad de México, D.F., México

A. Bedolla-Jacuinde
Instituto de Investigación en Metalurgia y Materiales, Universidad Michoacana de San Nicolás de Hidalgo, C.P. 58000, Morelia, México

H.A. González-Rojas
Department of Mechanical Engineering (EUETIB), DEFAM Group, Universitat Politécnica de Catalunya, 08034 Barcelona, Spain

M.A. Espinosa-Medina[a)]
Facultad de Ingeniería Mecánica, Universidad Michoacana de San Nicolás de Hidalgo, C.P. 58000, Morelia, México

(Received 9 February 2016; accepted 15 June 2016)

The effect on the mechanical properties at room temperature of Li and Ag additions to the Fe–Al (40 at.%)-based alloy produced by conventional casting were evaluated in this work. Alloying elements were added into a previously molted Fe–(40 at.%) aluminum-based alloy, stirred, and then cast into sand molds to directly produce tensile specimens. To determine the mechanical properties, tensile tests and hardness measurements were performed. The additions of both Ag and Li showed an increase in ductility and tensile strength of the intermetallic alloys. In addition, hardness was substantially increased with the Li addition. Lithium additions promoted a solid solution hardening, whereas 3 at.% of Ag additions promoted ductility due to a microstructural modification and to the formation of a soft Ag_3Al phase. Characterization by both optical and electronic microscopy, energy dispersive spectroscopy microanalysis, and x-ray diffraction supported the mechanical characterization.

I. INTRODUCTION

In the past, the Fe–Al-based intermetallic alloys had been studied with interest due to their excellent corrosion resistance and their potential application as structured materials at elevated temperatures in hostile environments in the energy conversion industries as: geothermal or fossil fuels and nuclear fuels to generate electrical power systems.[1–7] However, the use of those alloys as structural components had been limited due to their brittle fracture behavior and low ductility properties at room temperatures resulting from environmental embrittlement, weak grain boundaries, vacancy hardening, and embrittlement.[7] Environmental embrittlement involves moisture in air, which is the major cause of low tensile ductility. Such environmental embrittlement is the consequence of a chemical reaction involving the reaction of Al with oxygen from moisture, releasing hydrogen atoms that could be absorbed.[8] However, there are other factors that can modify mechanical behavior at room temperature, such as grain size, improving ductility as the grain size is reduced.[9] The quantity of Al in the FeAl alloy systems also has an important effect on both the mechanical properties[10] and corrosion resistance at high temperature applications.[7] For reason of this, a best condition for those properties for high temperature applications has been reported for Al concentrations between 35 and 45 at.%.[7,10–12] This has become the baseline for the production of those alloys.

Hence, the production of alloys by conventional melting techniques such as air-induction melting, vacuum-induction melting, vacuum-arc melting are applicable to melt and obtain intermetallics with different levels of purity is of industrial interest due to its relative low cost.[13] From above, first technique is the most economical technique. In those techniques, the kind of crucibles; the melting atmospheres applied (air, inert gas, vacuum); furnace loading of low

Contributing Editor: Jürgen Eckert
[a)]Address all correspondence to this author.
e-mail: marespmed@gmail.com
DOI: 10.1557/jmr.2016.249

 © Materials Research Society 2016

https://doi.org/10.1557/jmr.2016.249 Published online by Cambridge University Press

and high-melting-point metals between others, need to be considered. Exo-Melt™ process for melting[14,15] had been applied to process Ni and Fe aluminides with higher quality, by modifying the furnace-loading sequence to initiate the highly exothermic aluminide reaction to form superheated (Ni, Fe)–Al liquid. On the other hand, powder metallurgy technology described with the application of thermo-mechanical processing including sintering, cold rolling, annealing, and heat treating,[16,17] and the atomization and deposition procedure[18] consisted in to feed the master alloy casting previously obtained in the spray atomization and deposition system; to obtain a fine-grain structure in both cases.

In that sense, the induction melting and casting processing is one of the procedures that is also used for producing these FeAl alloys[7,10–19] and it could be sequenced by work-hardening[10,12] and/or heat treatment[11,19] processes to change the mechanical properties of the base alloy. In addition, alloying with ternary element additions is also useful for improving mechanical properties and hot corrosion resistance. The alloying process during melting is a very easy way to incorporate a third chemical element (or compound), which can be incorporated in solid solution[20] and/or partially, to form a secondary phase, usually like a segregated phase on the grain boundaries. The effect of alloying Fe–Al by third elements on the mechanical properties at room temperature has been studied before[4,5,19–27] with different results. Furthermore, the alloying effects on those mechanical properties of both the grain refinement and the environmental interaction have been evaluated.[21,22,26–29]

In this way, the alloying effect on the mechanical properties at room temperature of materials produced by the induction melting process becomes very interesting. Hamana et al.[19] reported that the raise of Cr additions to a Fe–28 at.% Al stabilized the B2 phase of the microstructure, which, in turn, increased its hardness when a heat treatment was applied, due to the modification of the B2 to $D0_3$ transition rate. Similarly, grain size modification,[23] third phase formations, and carbide precipitation[22,24] are important factors for improving mechanical properties. Salazar et al.[25] observed a notable upswing in ductility under compression tests at room temperature when Li was added to an FeAl intermetallic. Rosas et al.[21] have also reported a rise in ductility when adding Li to an Fe_3Al-based alloy, but under tensile loads. However, the effect on the mechanical properties by adding Ag to an FeAl-based alloy has not been reported. As the first step for a future high temperature assessment, the effects on the mechanical properties at room temperature of Li and Ag additions to an Fe–40 at.% Al-based alloy, produced by conventional casting, were evaluated in this work. The alloys were metallographic and chemically characterized by light microscopy, scanning electronic microscopy (SEM), x-ray diffraction, and energy dispersive spectroscopy (EDS).

II. EXPERIMENTAL PROCEDURE

The experimental alloys were produced in an induction furnace by using a silicon carbide crucible.[30] To produce Fe–40 at.% Al-based intermetallic alloys with additions of 1 and 3 at.% of Li and Ag, high purity raw materials were used (99.9% of purity). Table I summarizes the designed atomic chemical composition of the intermetallic cast alloys without considering the carbon content acquired from crucible due to this crucible type tends to contaminate the AlFe alloys with small amounts of carbon.[25] In accord with Salazar et al.,[25] a 0.053 wt% of carbon contents was measured in a Fe(40 at.%)Al + 1Li(at.%) forming carbides, mainly $AlFe_3C$. Carbon contamination was not measured here; however, it is expected to find some carbides traces in the FeAl-based alloys here characterized by x-ray results; it is discussed in results and discussion section. An Inductotherm induction furnace using an argon protection atmosphere was used to cover the liquid iron, and aluminum was then added and mechanically stirred. Finally, the third element was added, followed by a stirring for full dissolution and homogenization. To avoid losses by evaporation, the addition of Li was realized using an aluminum capsule to minimizing the spontaneous reaction of Li in the casting. The melt was cast into sand molds to produce next-to-shape tensile specimens directly from casting. Mechanical properties were measured by tensile tests according to the ASTM E8 standard.[31] They were carried out on a Shimadzu (UH-300kNI) universal testing machine (Shimadzu Scientific Instruments, Columbia, Maryland) at a strain rate of 0.4 mm/min. Hardness was measured in a Shimadzu (HMV-2) hardness tester by applying 100 g of load for 20 s with a diamond indenter.[32] Prior to the mechanical characterization, intermetallic alloys were isothermally heat-treated at 800 °C for 48 h to reduce the adsorbed hydrogen contents, and removing or stabilizing quenched-in vacancies also, as was described before,[13,20] however, that effect of the heat treatment over those was not measured.

Samples with a size close to 10 × 10 × 5 mm were cut from the castings, grinded to 1.0 μm grades with emery paper up to 1000 grind size, polished with 0.5 μm diamond particle suspension, and then etched for

TABLE I. Chemical composition of intermetallic alloys.

Designed $Fe_{60}Al_{40}$-based alloy	+at.% Li	+at.% Ag
Alloy-A	...	...
Alloy-B	1	...
Alloy-C	3	...
Alloy-D	...	1
Alloy-E	...	3

https://doi.org/10.1557/jmr.2016.249 Published online by Cambridge University Press

metallographic characterization. Chemical etching was performed using Keller's etchant (HCl, HNO_3, HF, and H_2O).[33] Stoichiometric characterization of the phases present in each alloy was determined by x-ray diffraction patterns, using Cu K_α radiation in a two-theta range from 20° to 110° in a SIEMENS 5000 diffractometer (Siemens Aktiengesellschaft, Munich, Germany). Optical microscope observation was done using a Nikon Epiphot 300 (Nikon Corporation, Tokyo, Japan) equipped with a digital camera for imaging. SEM was performed for imaging characterization and microanalysis by EDS in a Phillips ESEM-XL30 (FEI Company, Hillsboro, Oregon) equipped with an EDAX.

III. RESULTS AND DISCUSSION

A. Microstructural and chemical characterization

The macrostructure of the as-cast Fe–(40at.%Al)-based alloys was modified with the addition of a third alloying element. Figure 1 shows the optical image of metallographies at low magnifications of the base alloy and FeAl with 3 at.%Li and 3 at.%Ag (Alloy-A, Alloy-C, and Alloy-E). The base FeAl intermetallic showed a columnar grain distribution from the periphery toward the center bar in the opposite direction of the heat flow [Fig. 1(a)]. This characteristic morphology was identified (and described further ahead) with a low amount of the Fe_3Al phase homogeneously distributed into the FeAl matrix. The addition of Li to the base alloy improved a change in the appearance of the solidified macrostructure. The main observation was the modification of macro-grains: they changed from a columnar to an equiaxial shape; it is suggested that they formed due to a higher nucleation process during solidification. Thus, it was to be expected when equiaxed grains formed at the end of the solidification (in the center of the bar) and the percentage of this solidification mode was proportional to the quantities of Li addition [Fig. 1(b)]. A similar behavior was shown by the alloys with Ag addition (1, 3 at.%) [Fig. 1(c)]. However, those alloys showed a third phase formation, a singular phase containing high amounts of Ag and Al, almost at 3:1 ratio. This third phase increased with the addition of Ag [Fig. 1(c)].

Figure 2 shows the detailed microstructure of all alloys observed by SEM at higher magnifications. Figure 2(a) displays the morphologies of the structural phases of the base FeAl. The base alloy was composed of two phases: the small amount of the Fe_3Al phase homogeneously dispersed into the major phase of FeAl, as described above, and in agreement with the x-ray diffraction results and EDS [Fig. 2(b)][30] The minor phase showed size variations, up to 20 μm in length and an average width of 3–7 μm. The minor phase solidified as a dendritic mode with primary and secondary arms of around 5 μm in diameter. Li additions promoted the modification of such a type of morphology and decreased the amount of the Fe_3Al minor phase [Figs. 2(c) and 2(d)]. It was suggested that this decrease was caused by an

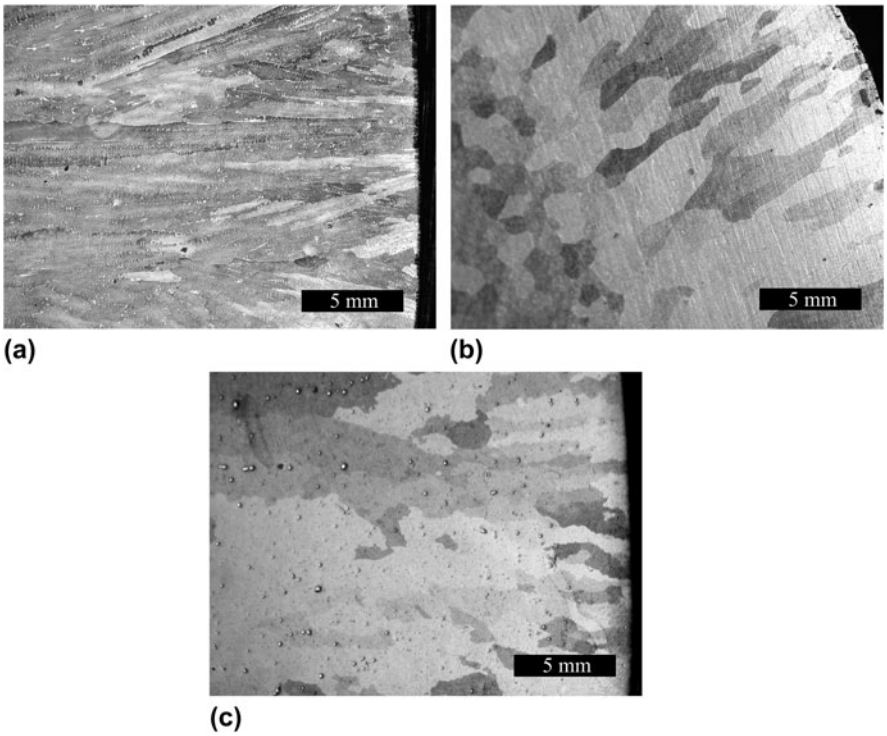


FIG. 1. Metallographic images observed by light microscopy of (a) Alloy-A, (b) Alloy-C, and (c) Alloy-E.

https://doi.org/10.1557/jmr.2016.249 Published online by Cambridge University Press

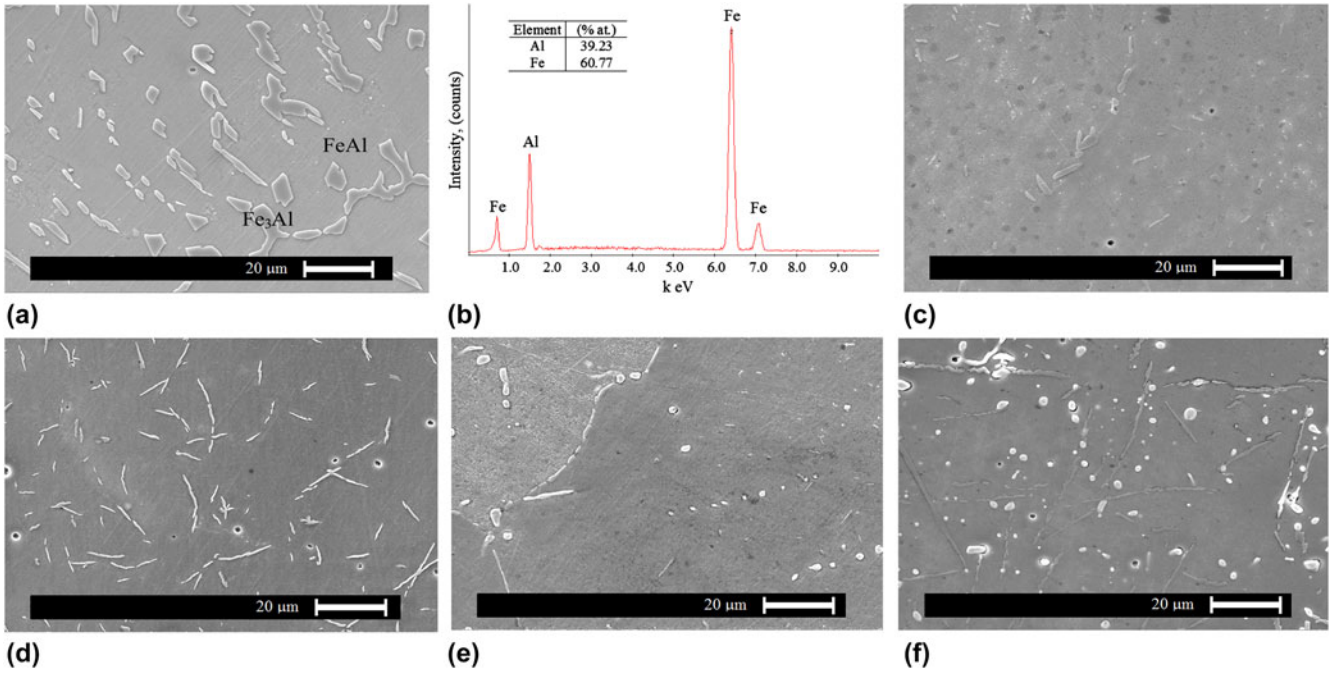


FIG. 2. SEM micrographs observed for (a) Alloy-A, (b) EDS chemical analysis of Alloy-A, (c) Alloy-B, (d) Alloy-C, (e) Alloy-D, and (f) Alloy-E.

incorporation of solid solution, according to the x-ray diffraction results.[30] On the other hand, Ag additions promoted the formation of a third phase, identified as an Ag_3Al intermetallic compound. Similar to the Li additions, the Ag alloying promoted the modification of the microstructural morphology by decreasing the amount of Fe_3Al [Figs. 2(e) and 2(f)] and, in turn, increasing the amount of Ag_3Al.

The EDS analysis carried out for all the observed phases showed the semiquantitative stoichiometry of the compounds. Those analyses corresponded to the atomic ratio of the FeAl, Fe_3Al, and Ag_3Al intermetallic compounds verified by x-ray diffraction (described further ahead). The SEM characterization showed that the second phases in the base FeAl alloy presented a quasiregular distribution [Fig. 2(a)]. Additions of Li led to a refinement of the minor phase, showing a uniformly distributed needle shape [Fig. 2(c)]. X-ray diffraction results did not present patterns of Li or Li compounds; we suggest that Li remains in solid solution into the base alloy. Also, close to 0.5 at.% of Ag was incorporated in solid solution in the FeAl + Ag (1, 3 at.%) alloys. In those alloys, the excess of Ag concentration segregated toward the solidification front, as Ag_3Al [Figs. 2(e) and 2(f)]. Similarly, the Fe_3Al phase was refined and showed a needle shape, as did the FeAl + Li alloy. The effect of the third alloying element (Li and Ag) on the refinement of the Fe_3Al phase could be due to the ability of iron to occupy sublattice sites, originally occupied by aluminum, through an excess of iron atoms. This is known as the antisite defect.[6] It is suggested that microalloying may promote a decrease in the occupied sites by Fe in the FeAl B2 lattice, hence decreasing the Fe contents for Fe_3Al formation, which, in turn, decreases the amount of this latter phase.

Figure 3 shows the x-ray diffraction patterns obtained for the FeAl-based alloys according to PCPDF-based data patterns: 28-0034 (Ag_3Al), 65-6132 (FeAl), and 65-5188 (Fe_3Al). Alloy A (base FeAl) shows the presence of a carbide phase with a stoichiometry composition given by $AlFe_3C_{0.5}$ (PDF 29-0044 pattern) only observed in this alloy. The presence of this carbide phase was related to the carbon content, as reported before.[25] The FeAl and Fe_3Al phases had similar reflections of principal peaks, but different plane orientations. The planes associated to these peaks were (220) for Fe_3Al and (110) for FeAl around at 45°, while they were (400) for Fe_3Al and (200) for FeAl at 65° approximately. The $AlFe_3C_{0.5}$ had two main peaks related to the planes (111) and (200). Similarly, Alloy-B and Alloy-C showed FeAl and Fe_3Al phases, but not other phase formations when Li was added as carbides compounds. The FeAl+3Li had a remarkable intensity increment in the peaks at 32 and 65° approximately; those associated to the planes (100) and (200) respectably, whereas there was an intensity decrement in the peak at 45°. Therefore, these modifications in the intensity of the main reflection, we suggested that this element entered into the solid solution, and its effect was reflected on the microstructure and mechanical properties (last are discussed later). However, one of the main effects of the alloying additions to the FeAl-based alloys is related with the appreciable reduction of the carbides presence.[25]

https://doi.org/10.1557/jmr.2016.249 Published online by Cambridge University Press

On the other hand, Ag additions to the base FeAl (Alloy-D and Alloy-E) did indeed promote an Ag-rich phase formation during the solidification process, identified as Ag_3Al (Fig. 3). Figure 4, shows the EDS spectra of the FeAl + Ag matrix and the segregated particles of the Ag-rich phase. The matrix showed limited Ag solubility, between a 0.4 to 0.6 Ag at.% content [Fig. 4(a)], whereas the segregated phase showed higher amount of Ag. The Ag additions had two types of interactions with the base FeAl alloy. An amount of approximately 0.5 at.% Ag atoms entered into the B2 crystalline lattice through the substitutional solid solution [Fig. 4(a)], and the remaining amount of Ag was segregated toward the solidification front, forming the Ag_3Al phase [Fig. 4(b)]. A similar effect has been observed with Mo addition to a FeAl due to the Mo_3Al phase formation.[4]

Due to x-ray diffraction, patterns did not show any carbide existence in the alloys with third element addition (Fig. 3), the existence of $AlFeC_{0.5}$ can not be discarded; but the carbon and the carbide formation in those alloys could be reduced with third alloy elements[21,25] at concentrations not measurable with this tool. In this work, Li and Ag were used to improve the mechanical properties in a Fe–40 at.% Al alloy, and both elements diminished the carbon contents, around 75% with 1 at.% Li addition in base FeAl alloy.[25]

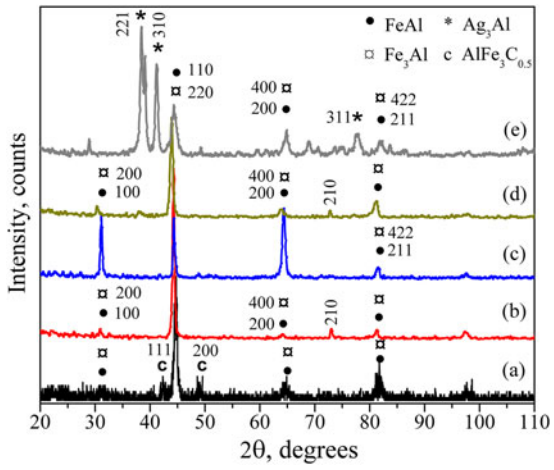


FIG. 3. X-ray spectra obtained on the FeAl-based and FeAl + (Li, Ag) intermetallic alloys (summarized in Table I).

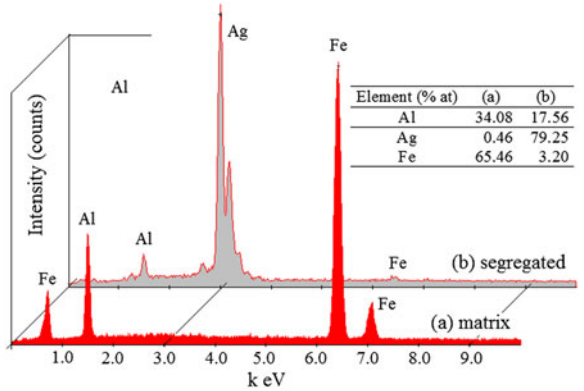


FIG. 4. EDS chemical analysis of FeAl with Ag additions (a) matrix phase and (b) Ag-rich segregated phase (segregated from Alloy-D).

The intensity changes of diffraction peaks was observed with the third element addition (Fig. 3), The intensity peak around 45° increased for 1Li as before reported,[21] whereas for both 3Li and 3Ag additions, the peak intensity decreases but increases at 65°. The study case in this work showed the FeAl-1Li had similar peaks as previously reported for an Fe_3Al alloy with 1 at.% Li identified at the 2θ angles: 32° 45°, 65°, 82° (diffraction planes: 200, 220, 400, 422, respectively).[21] The explanation for these changes was that the additions of the third alloy element could modify the preferential orientations along certain axes. In this sense, the Li addition effects were associated to an expansion of unit cell[34] as a microstructure and multiplicity factors by the peak diffraction on the (100) and (200) planes (at 32 and 65°), due its solid solution ingress.

B. Mechanical characterization

The addition of both Ag and Li to the FeAl-based alloy promoted some changes in the mechanical properties. Both elements improved the ductility in terms of elongation change percentage, and tensile strength of the base alloy, as well as the hardness. Addition of third element improved the elongation around 35, 85, and 130% for 1Li, 3 Li and 3Ag versus the showed by base alloy (which present a 0.31% in its plastic elongation); but 1 at.% Ag did not cause apparent ductility. A previous report on the mechanical evaluation of an FeAl (36.5% Al) alloy showed brittle cleavage fracture and only 2.2% tensile elongation when tested in air at room temperature, but the same alloy tested in a conventional vacuum had a ductility of about 8%.[7] The addition of Li to the base FeAl improved the solid solution hardening effect, which is suggested to be due to the modification of red parameter by expansion[34] and effect of carbon addition by contamination from SiC crucible, as similar effect as carbon or Mo.[4,35] The x-ray results show evidence of the precipitation of $AlFe_3C_{0.5}$ carbides in the alloy A, but no evidence was observed in the alloys with Li and Ag additions. Therefore, the $AlFe_3C_{0.5}$ presence is due to an interaction between the melted alloy elements and the SiC crucible.[25] The use of SiC crucibles is a very common practice in alloy casting such as the technique used in this work. Although the $AlFe_3C_{0.5}$ was not planned to be obtained, the carbide compounds could benefit the mechanical strengthening[22] and ductility.[13] Plots of tensile results are shown in Fig. 5, and some mechanical parameters from hardness and tensile measurements are summarized in Table II. Yield strength of a brittle material was calculated

https://doi.org/10.1557/jmr.2016.249 Published online by Cambridge University Press

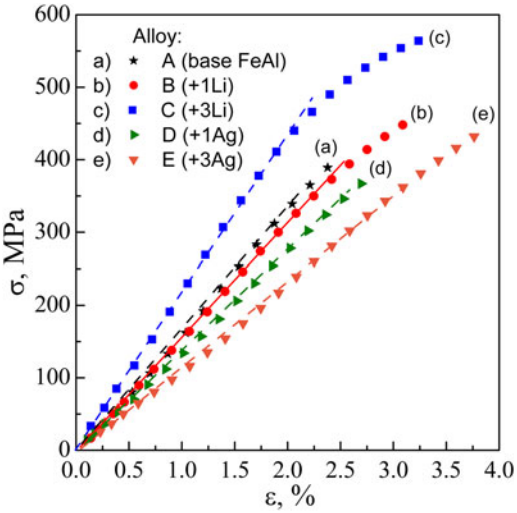


FIG. 5. Strength–strain plots of tensile test from FeAl-based alloys.

TABLE II. Strength–strain parameters (σ, ε) and hardness measurements of FeAl-based alloys.

Alloy	Hardness (Hv), MPa	*E* module MPa	UTS, MPa
Alloy-A	379.8	16,703	390
Alloy-B	432.6	15,531	448
Alloy-C	476.0	21,773	568
Alloy-D	323.8	13,793	366
Alloy-E	363.8	11,569	433

with the ultimate tensile strength (UTS), as recommended by the ASTM E8 standard.[31]

The FeAl-based alloy presented a UTS value of 390 MPa in air at room temperature (Table I). Morris et al.[10] have reported that yield stress increases with Al content up to 25%, and it decreases rapidly in the 25–28% Al range, but shows increment over the 30–40% Al range. They described ductility as an inverse relationship to the yield stress, with a rapid fall in ductility up to 25% Al, a slight maximum at 28% Al, and a steady, slow fall thereafter. The yield stress and ductility of the base FeAl in the present work are in agreement with the observations of Morris et al.[10] Besides, it was in according with the 360 MPa strength value at room temperature for the B2 structured Fe–45Al–4Cr–0.1Zr–0.02B alloy, melted in vacuum and homogenizing at 1000 °C/72 h, reported by Kupta[11]; however it was tested in an argon atmosphere. In our work, the additions of Li to the FeAl-based alloy improved the mechanical properties, showing UTS values of 448 and 568 MPa (Fig. 5) and elongation increasing between 35 and 85% for Alloy-B and Alloy-C, respectively versus base alloy. Similar upswings of UTS values of FeAl alloys have been obtained with additions of carbon[35] or molybdenum.[4] Salazar et al.[25] reported similar effects when adding Li to a similar alloy, but tested under compressive stress. The effects of Ag additions were more meaningful in the elongation results, increasing around 130% for 3Ag (at.%), respectively. However, a small increase in UTS values was observed, around 366 and 433 MPa (Fig. 5; Alloy-4 and Alloy-5).

C. Fractographic characterization

The results of mechanical strength and hardness showed a direct correlation with Li addition contents, but this was not seen in relation to elongation, which was similar at the 1 and 3% Li content. On the other hand, Ag additions did not significantly improve strength. However, elongation was higher than the one of the added lithium alloys, particularly the alloy with 3 at.% of Ag. Ductility in the FeAl + Ag systems was affected in proportion to the Ag addition. This effect is explained in terms of the third phase formed in the alloys, which allowed the plastic displacement among the grain faces of both the FeAl and Ag_3Al phases (Fig. 2). In this sense, fracture morphology of the tensile tests provided more evidence of the plasticity or hardening effect of the Li and Ag additions. Figure 6 shows the SEM images of the resulting fractographs of the tensile tests of the FeAl-based alloys.

The effect of the third element addition on the improvement of elongation was more evident with 3Ag and 3Li additions rather than 1Li was added. Namely, the maximum elongation % at strain condition was increased by Alloy-E (around 85% versus base FeAl), whereas (1, 3 at.%) Li addition promoted an increasing change of around 35 and 85%. However, characteristic brittle fractures were observed on all alloys (Fig. 6). Alloy-A showed intergranular failure mode by grain decohesion [Fig. 6(a)], associated with ⟨111⟩ or ⟨100⟩ slips,[6] but it was modified by the third alloying additions, particularly with the Ag additions. Due to the plasticity improvement of the Ag additions, the fracture mode was changed from only intergranular to a mixture of intergranular and transgranular fracture [Figs. 6(d) and 6(e)]. On a minor level, Li additions promoted a fraction of transgranular fracture mode mixed with intergranular decohesion of the strongly anchored columnar grains, as an effect of the increase in strength [Figs. 6(b) and 6(c)]. This long intergranular failure mode occurred parallel to the columnar grain length.

FeAl intermetallic alloys did not show an apparent yield point discontinuity on the tensile tests (Fig. 5). This behavior is typical of brittle alloys. However, some level of ductility was evidenced by the change in the percent of elongation at strain condition with the 3Ag addition (Fig. 6) and the characteristic fracture mode. The change in the fracture mode for these alloys showed a transition from intergranular to transgranular and cleavage fracture, as previously reported.[27] That fracture mode was caused by the addition of ternary elements, and in this way the effect of Li represented an increase of around 44% in

https://doi.org/10.1557/jmr.2016.249 Published online by Cambridge University Press

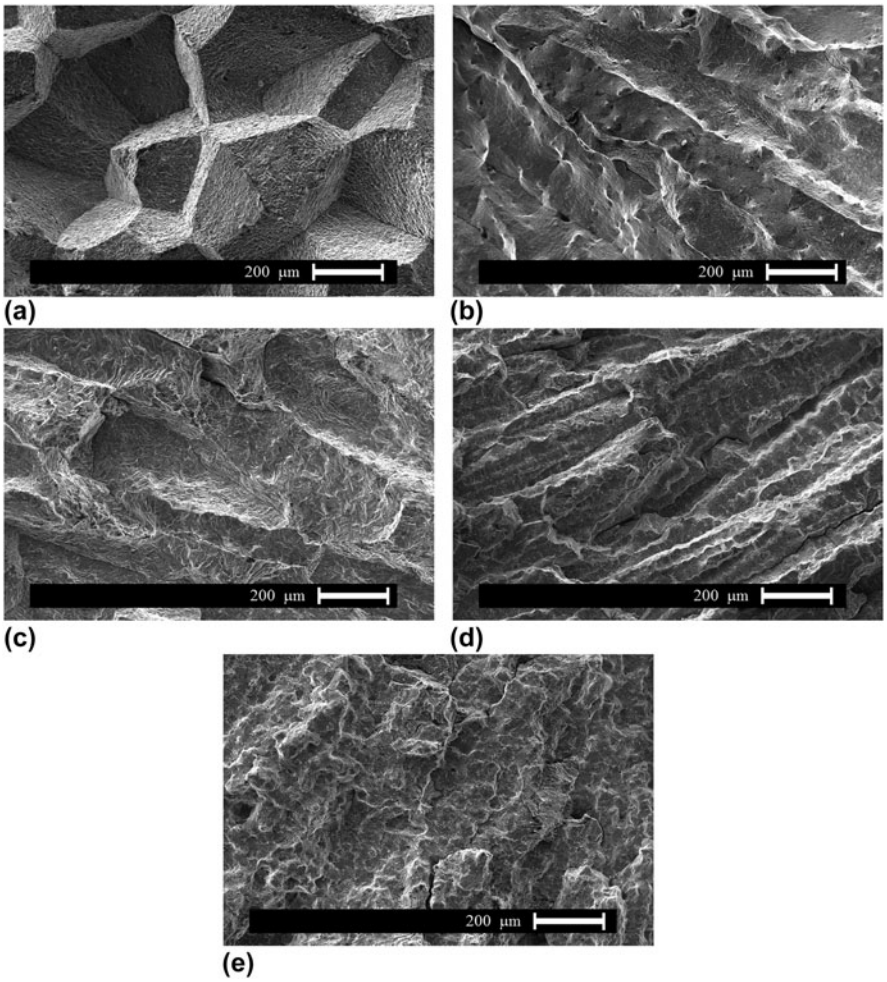


FIG. 6. SEM images at ×100 magnification of specimens fractured by the tension test of: (a) Alloy-A, (b) Alloy-B, (c) Alloy- Alloy-C, (d) Alloy-D, and (e) Alloy-E.

the UTS. Although tensile tests were not carried out in a controlled environmental atmosphere, the results could be comparable to those obtained when studying the effect of the environment and the strain rate on tensile properties of FeAl crystals by Wu and Baker.[29] In addition, those results also concur with the results obtained by Pike and Liu,[26] who studied the effect of vacancies on the environmental yield strength dependence of boron-free and boron-doped Fe–40Al. They reported an increase of almost 200 MPa of UTS on tests carried out in a vacuum, compared with the same alloys tested in air. The UTS values of the vacuum tests are similar to the UTS value shown by the Alloy-C in the present work. The Ag addition alloys (Alloy-D and E) showed a small effect on UTS behavior and the rise in the percentage of transgranular fracture, which evidences cleavage facets promoted by the presence of the Ag_3Al ductile phase, has also been previously observed.[28]

The change in the ductility of the base FeAl alloy represented by an increase in the elongation percentage is attributed to the modification of the microstructures. Similar results were reported by Huang[22] and Chao et al.[28] The former studied the influence of microstructure and test conditions on the tensile behavior of FeAl-based alloys with Mo, Nb, Zr, and C, which effectively improved the strength properties.[22] The latter analyzed that influence with Y_2O_3 particles (18 and 150 nm) and found that the major changes of strength were obtained by the grain refinement. They reported an increase of ductility of about 10% associated with grain size ranging from 1 to 100 μm.[28] Of course, the environmental control and surface finishing of the samples were very closely controlled. In the present work, the strengthening modification was attributed to the microstructure refinement in the base FeAl by the Li addition through redistribution and shape modification of the Fe_3Al phase (Fig. 2). The increase in hardness was associated with the microstructural modifications by means of the combined contributions of vacancy hardening into an ordered and disordered domain/particle between grain borders and phases generated by the Li addition.[36] On the other hand, the softening effects due to the Ag additions were associated with the

https://doi.org/10.1557/jmr.2016.249 Published online by Cambridge University Press

decreased Fe_3Al phase and the formation of the third Ag_3Al phase. In that case, the ordered and disordered vacancy hardening was not associated with the decrease of hardening, but was related to the third soft phase, which enhanced the plastic behavior. These results are in agreement with those reported by Cielsar et al.,[24] who studied the influence of Cr and Ce additions on the mechanical properties of the Fe–(28 at.%)Al system, which promoted the precipitation of Cr–Fe–(C) particles, decreasing the hardness of the alloy with Cr content. In summary, the additions of Li and Ag to the Fe–(40 at.%) Al-based alloys increased the tensile strength at room temperature, due to the contribution of both the solid solution hardening and the vacancy increasing in the microstructures. Additionally, the change in ductile behavior was promoted by the microstructural changes, which had an important effect on slip plains, but the main contribution was attributed to the formation of the soft Ag_3Al phase in the Ag content alloys.

IV. CONCLUSIONS

The additions of both Ag and Li into the FeAl-based alloy led to modify ductility and tensile strength. Li promoted a direct increase on strength and hardness due to solid solution hardening effects, and improvement in ductility for both additions. On the other hand, Ag additions did not significantly improve the strength properties. However, this addition promoted an elongation higher with 3 at.% addition than 1 at.% similar to 1 at.% Li effect.

Changes in the fracture mode were also observed when alloying the FeAl. The change in the fracture mode for these alloys showed a transition from intergranular to transgranular and cleavage fracture. Li additions caused an approximately 50% increase in the UTS, whereas a lower effect was shown by the Ag addition. Additionally, Ag additions could rise the percentage of transgranular fracture due to the presence of the ductile phase.

Additions of Li and Ag to the Fe–(40 at.%)Al-based alloys increased the tensile strength at room temperature due to the contribution of both the solid solution hardening and the vacancy increasing in the microstructures. Additionally, the increase in ductility was promoted by the microstructural change, which had an important effect on slip planes, but the primary contribution was attributed to the formation of the soft Ag_3Al phase in the $Fe_{60}Al_{40}$–(1,3)Ag alloys.

ACKNOWLEDGMENTS

The present research was supported by CONACYT for the project financing Number: 243236, CB-2014-02, I0017 Fund.

REFERENCES

1. F. Charlot, E. Gaffet, B. Zeghmati, F. Bernard, and J.C. Niepce: Mechanically activated synthesis studied by x-ray diffraction in the Fe–Al system. *Mater. Sci. Eng., A* **262**, 279 (1999).
2. M. Kupka: Technological plasticity studies of the FeAl intermetallic phase-based alloy. *Intermetallics* **12**, 295 (2004).
3. W.J. Zhang, R.S. Sundar, and S.C. Deevi: Improvement of the creep resistance of FeAl-based alloys. *Intermetallics* **12**, 893 (2004).
4. M. Eumann, M. Palm, and G. Sauthoff: Alloys based on Fe_3Al or FeAl with strengthening Mo_3Al precipitates. *Intermetallics* **12**, 625 (2004).
5. A.O. Mekhrabov and M.V. Akdeniz: Effect of ternary alloying elements addition on atomic ordering characteristics of Fe–Al intermetallics. *Acta Mater.* **47**, 2067 (1999).
6. I. Baker and P.R. Munroe: Mechanical properties of FeAl. *Int. Mater. Rev.* **42**, 181 (1997).
7. C.T. Liu, E.P. George, P.J. Maziasz, and J.H. Schneibel: Recent advances in B2 iron aluminide alloys: Deformation, fracture and alloy design. *Mater. Sci. Eng., A* **258**, 84 (1998).
8. N.S. Stoloff and C.T. Liu: Environmental embrittlement of iron aluminides. *Intermetallics* **2**, 75 (1994).
9. I. Baker, O. Klein, C. Nelson, and E.P. George: Effects of boron and grain-size on the strain-rate sensitivity of Fe–45Al. *Scr. Metall. Mater.* **30**, 863 (1994).
10. D.G. Morris, M.A. Munoz-Morris, and L.M. Requejo: Work hardening in Fe–Al alloys. *Mater. Sci. Eng., A* **460–461**, 163 (2007).
11. M. Kupka: Temperature dependence of the yield stress of an FeAl base alloy. *Mater. Sci. Eng., A* **336**, 320 (2002).
12. L. Pang and K.S. Kumar: Mechanical behavior of an Fe–40Al–0.6C alloy. *Acta Mater.* **46**, 4017 (1998).
13. S.C. Deevi and V.K. Sikka: Nickel and iron aluminides: An overview on properties, processing, and applications. *Intermetallics* **4**(5), 357 (1996).
14. S.C. Deevi and V.K. Sikka: Exo-MeltTM process for melting and casting intermetallics. *Intermetallics* **5**(1), 17 (1997).
15. V.K. Sikka, D. Wilkening, J. Liebetrau, and B. Mackey: Melting and casting of FeAl-based cast alloy. *Mater. Sci. Eng., A* **258**, 229 (1998).
16. R.E. Mistler, V.K. Sikka, C.R. Scorey, J.E. McKernan, and M.R. Hajaligol: Tape casting as a fabrication process for iron aluminide FeAl thin sheets. *Mater. Sci. Eng., A* **258**, 258 (1998).
17. M.R. Hajaligol, S.C. Deevi, V.K. Sikka, and C.R. Scorey: A thermomechanical process to make iron aluminide FeAl sheet. *Mater. Sci. Eng., A* **258**, 249 (1998).
18. L. Martinez, M. Amaya, J. Porcayo-Calderon, and E.J. Lavernia: High-temperature electrochemical testing of spray atomized and deposited iron aluminides alloyed with boron and reinforced with alumina particulate. *Mater. Sci. Eng., A* **258**, 306 (1998).
19. D. Hamana, L. Amiour, and M. Bouchear: Effect of chromium ternary additions on the ordering behaviour in Fe–28 at.% Al alloy. *Mater. Chem. Phys.* **112**, 816 (2008).
20. J.H. Schneibel: Strengthening of iron aluminides by vacancies and/or nickel. *Mater. Sci. Eng., A* **258**, 181 (1998).
21. G. Rosas, R. Esparza, A. Bedolla-Jacuinde, and R. Perez: Room temperature mechanical properties of Fe_3Al intermetallic alloys with Li and Ni additions. *J. Mater. Eng. Perform.* **9**, 57 (2009).
22. Y.D. Huang and L. Froyen: On the effect of microstructural parameters on tensile properties of a high work-hardening Fe_3Al-based alloy. *Intermetallics* **11**, 361 (2003).
23. A. Wasilkowska, M. Bartsch, F. Stein, M. Palm, G. Sauthoff, and U. Messerschmidt: Plastic deformation of Fe–Al polycrystals strengthened with Zr-containing laves phases—Part II. Mechanical properties. *Mater. Sci. Eng., A* **381**, 1 (2004).

https://doi.org/10.1557/jmr.2016.249 Published online by Cambridge University Press

24. M. Cieslar, M. Karlık, M. Benko, and T. Cernoch: The influence of Cr and Ce additions on the mechanical properties of Fe_3Al based alloys. *Mater. Sci. Eng., A* **324**, 23 (2002).
25. M. Salazar, A. Albiter, G. Rosas, and R. Perez: Structural and mechanical properties of the AlFe intermetallic alloy with Li, Ce and Ni additions. *Mater. Sci. Eng., A* **351**, 154 (2003).
26. L.M. Pike and C.T. Liu: The effect of vacancies on the environmental yield strength dependence of boron-free and boron-doped Fe–40Al. *Intermetallics* **8**, 1413 (2000).
27. P. Hausild, M. Karlik, J. Siegl, and I. Nedbal: Fractographic analysis of the crack growth in the Fe_3Al based intermetallic alloy. *Intermetallics* **13**, 217 (2005).
28. J. Chao, D.G. Morris, M.A. Muñoz-Morris, and J.L. Gonzalez-Carrasco: The influence of some microstructural and test parameters on the tensile behaviour and the ductility of a mechanically-alloyed Fe–40Al alloy. *Intermetallics* **9**, 299 (2001).
29. D. Wu and I. Baker: The effect of environment and strain rate on the room temperature tensile properties of FeAl single crystals. *Intermetallics* **9**, 57 (2001).
30. J.C. Romo Castañeda: *Thesis: Characterization of a FeAl* (Facultad de Química, Universidad Nacional Autónoma de México, México City, 2006).
31. ASTM Designation: E 8M: *Standard Test Methods for Tension Testing of Metallic Materials* [Metric] (2001).
32. ASTM Designation: E3: *Standard Guide for Preparation of Metallographic Specimens* (2001).
33. ASTM Designation: E 407: *Standard practice for Microetching metals and alloys* (1999).
34. Y. Yang, H. Masaaki, Y. Masao, and K. Ryoji: Synthesis, crystal structure, and electrode characteristics of $LiMnPO_4(OH)$ cathode for lithium batteries. *J. Solid State Chem.* **187**, 124 (2012).
35. R.G. Baligidad and A. Radhakrishna: Effect of carbon and processing on structure and mechanical properties of Fe-11 wt.% Al alloy. *Mater. Sci. Eng., A* **283**, 211 (2000).
36. X. Amils, J. Nogues, S. Suriñach, M.D. Baro, M.A. Muñoz-Morris, and D.G. Morris: Hardening and softening of FeAl during milling and annealing. *Intermetallics* **8**, 805 (2000).

https://doi.org/10.1557/jmr.2016.249 Published online by Cambridge University Press